

Research Article

Functional imaging in non-small cell lung carcinoma: Correlation between standardized uptake values and apparent diffusion coefficient valuesNecdet Poyraz¹, Cihan Şimşek¹, Celalettin Korkmaz², Buğra Kaya³, Hasan Emin Kaya¹¹Necmettin Erbakan University, Meram Faculty of Medicine, Department of Radiology, Konya, Turkey²Necmettin Erbakan University, Meram Faculty of Medicine, Department of Pulmonology, Konya, Turkey³Necmettin Erbakan University, Meram Faculty of Medicine, Department of Nuclear Medicine, Konya, Turkey**Corresponding author:** Necdet Poyraz,

Necmettin Erbakan University, Meram Faculty of Medicine, Department of Radiology, Konya, Turkey

Abstract:**Objective:** To investigate the relationship between apparent diffusion coefficient (ADC) values and standard uptake value (SUV) in patients with non-small cell lung cancer (NSCLC).**Methods:** PET/CT and diffusion-weighted magnetic resonance imaging (DW MRI) were performed in 73 consecutive patients with histologically verified NSCLC. Analysing the PET/CT data calculation of the maximum and mean SUV was performed. The mean and minimum ADC values were measured directly on the parametric ADC maps.**Results:** Significant inverse correlations were found between ADC_{mean} and SUV_{mean} ($r = -0.53$; $p < 0.001$) as well as ADC_{min} and SUV_{max} ($r = -0.71$; $p < 0.001$).**Conclusions:** The significant negative correlations between ADC and SUV suggest an association between tumor cellularity and metabolic activity in NSCLC.**Keywords:** Diffusion-weighted magnetic resonance imaging, Apparent diffusion coefficient, PET/CT, Non-small cell lung cancer.**INTRODUCTION**

Lung cancer is the most common cancer and one of the leading causes of cancer-related mortality worldwide (1), with non-small cell lung cancer (NSCLC) accounting for 80% of all new lung cancers. More than 80% of the lung cancers are non-small cell lung cancer (NSCLC) which affects about 1.35 million people in the world (2). The majority of the patients present with locally advanced or metastatic stage. Five-year survival rate is less than 9% in these patients and when all stages are considered, it is about 14%. Survival and response to treatment are multifactorial and affected by stage, performance status, and genetic factors (3). There are differences among patients with the same stage in terms of treatment response, recurrence, and survival rate. Thus, oncologists need some clinical and laboratory parameters to determine treatment strategies, evaluate prognosis and follow up in patients with newly diagnosed lung cancer (4).

Positron emission tomography-computed tomography (PET/CT) has become a preferred imaging modality in cancer diagnosis, staging, and treatment. Previous studies have shown that PET/CT provides information not only about tumor morphology but also about proliferation rate of the tumor and survival by showing the increased metabolic activity of tumor cells in patients with NSCLC (5-9). There are also studies

demonstrating that standard uptake value (SUV) of the primary tumor is an independent prognostic factor (7). Recently, the apparent diffusion coefficient (ADC), a parameter of magnetic resonance imaging (MRI) measured on diffusion-weighted imaging (DWI), has gained increasing attention as a diagnostic tool to determine tumor cellularity and aggressiveness (10,11). Both ADC and SUV are quantitative parameters to evaluate tumor malignancy, and several studies have attempted to demonstrate that ADC and SUV are negatively correlated in some types of cancers with high cellularity (12-14).

However, the correlation between ADC and SUV is not revealed in pancreatic cancer, which is known not only for its high malignancy, but also for tumor-induced fibrous changes, inflammatory reaction, and obstruction of pancreatic duct behind the scene. Matoba et al. reported that cellularity of lung tumors is inversely correlated with ADC values (13).

Although SUVs and ADC values have emerged as potential biomarkers, their relationship in NSCLC is not fully elucidated. The number of studies on this issue is limited and they have inconsistent results. One study in which 41 NSCLC patients are included, reported no correlations between the ADC_{mean} and the SUV_{max} or SUV_{mean} (15), whereas another study with 18 NSCLC patients reported a statistically significant inverse correlation between the SUV_{max} or SUV_{mean} and ADC_{mean} (16). Further studies are thus

needed to confirm the relationship between SUV and ADC in lung cancer.

The aim of this prospective study was, therefore, to investigate whether the correlation between the SUV derived by PET/CT and the ADC calculated on the basis of diffusion-weighted MRI in newly diagnosed NSCLC.

Materials and methods

MRI was performed (without IV contrast administration) in 94 consecutive patients with histologically proven NSCLC after routine clinical PET/CT in this prospective study. None of the patients had a previous malignant disease, received anticancer drugs or radiotherapy. PET/CT studies had been performed within 2 weeks prior to MRI for each patient. Patients with contraindications to MRI such as pacemakers, metal implants, claustrophobia were excluded.

The study protocol was approved by the Institutional Review Board and written informed consent was obtained from all subjects prior to the examinations.

PET/CT Imaging

All of the patients fasted for at least 4–6 hours and the blood glucose levels of the patients were measured before intravenous injection of 370 mBq (10 mCi) 18F-fluorodeoxyglucose (18F-FDG). PET/CT scans were obtained 60 minutes after the 18F-FDG injection using an integrated scanner (Siemens, Biograph 6 HiRes PET/CT). Whole body PET/CT images were acquired from the vertex to the upper thigh. CT scans were performed without intravenous contrast administration with 130kV, 50 mAs, a pitch of 1.5, 5 mm slice thickness and 70 cm field of view. PET scans were performed immediately after the unenhanced CT studies and images were acquired using a three-dimensional (3D) acquisition mode with a 3 minutes acquisition per bed position. In the PET attenuation correction, unenhanced CT data were used.

DW MRI

MRI was performed with 1.5-Tesla MR unit (Avanto, SIEMENS Systems, Erlangen, Germany) using a body phased array coil. Patients were imaged in the supine position throughout the examination. Conventional MRI included coronal T2-weighted BLADE sequence (repetition time 3040 msec, echo time 123 msec and 1 excitation) and axial T2-weighted HASTE sequence (repetition time 600 msec, echo time 31 msec and 1 excitation). Respiratory triggering was not used, DW MRI was obtained in the transverse plane during free breathing with single-shot echo planar read-out, using a spectral selection attenuated inversion recovery (SPAIR) technique for fat suppression. Motion-probing gradients were added to the three axes (axial, sagittal, and coronal) on DW images. All DWI examinations were performed within 12 minutes (mean examination time, 8.5 minutes; range, 7–12 minutes). DW sequence parameters are given in Table 1.

Table 1. Imaging parameters of the DWI sequence

Parameter	Value
Slice thickness	5 mm
Field of view	320*380 mm
Matrix size	115p*192
Repetition time	7,400 msec
Echo time	75 msec
Fat saturation	SPAIR
Parallel imaging	GRAPPA
Averages	2
b values	50, 800 sec/mm ²

GRAPPA Generalized autocalibration partial parallel acquisition, *SPAIR* Spectral selection attenuated inversion recovery

ADC values were calculated according to the following formula: $ADC = - (1 / b) \ln (S2 / S1)$, where the S2 and S1 are the signal intensities at b value of 800 and 50 s/mm², respectively. We used b values greater than 50 s/mm² to reduce the effects of perfusion on ADC estimation.

Image analysis

All the MR images were transferred to a workstation (Leonardo, Siemens Healthcare) and the ADC maps were automatically generated using two b-values (50 and 800 s/mm²). MR images were evaluated by two radiologists with 4 and 12 years of experience in thoracic imaging. The largest diameter lesion defined as the target lesion identified on axial T2-weighted HASTE sequence. For quantitative evaluation, a region of interest (ROI) was independently placed on the target lesion on a single axial ADC image obtained at a b-value of 800 s/mm². ADC measurements were made on ADC map best depicting the tumor by placing one small round (OSR) ROI on the most hypointense area of the tumor while avoiding necrotic-cystic areas and artifacts. The solid parts of the tumors were identified as areas with high signal intensity on DWI, matched hypointensity on ADC maps, and increased accumulation of 18F-FDG on PET/CT. ADC values were recorded as “mean ADC value” (ADC_{mean}) and the lowest values as “minimum ADC value” (ADC_{min}). The area of ROI ranged from 60 mm² to 80 mm² for OSR method as reported in a previous study (17). To ensure that the same lesions at the same levels were measured on MRI and PET/CT, the reports and the images of the PET/CT studies were available during data analysis on a separate workstation.

The corresponding 18F-FDG PET/CT images were reviewed on the PET/CT system’s workstation (TrueD, Siemens Medical Systems) by one nuclear medicine physician with 8 years of experience in reading whole-body PET/CT scans. First, 18F-FDG PET scans were reviewed and the index lesion was considered to be the largest lesion on axial CT scan with visually highest 18F-FDG uptake. For quantitative evaluation, a region of interest (ROI) was independently placed on the target lesion on a single axial slice of the PET/CT best depicting the tumor. Later, SUV_{max}, SUV_{mean} values of the

lesions with increased 18F-FDG uptake were calculated on PET/CT fusion images. SUV was calculated by the following formula: SUV (g/ml) = regional radioactivity concentration (Bq/ml)/[injected dose (Bq)/body weight (g)].

The time interval between SUV and ADC measurements was at least 7 days, and the reviewers were blinded to ADCs when measuring SUVs (and vice versa) and to the histopathological results.

Statistics

The Shapiro-Wilk test was used to check whether the SUV and ADC measurements were normally distributed. Subsequently, Pearson’s correlation coefficients were calculated between SUVmax and ADCmin, SUVmean and ADCmean. The inter-reader variability for ADC values were determined by the intraclass correlation coefficient (ICC, ranges and correlation: 0.00–0.20, poor; 0.21–0.40, fair; 0.41–0.60, moderate; 0.61–0.80 good; 0.81–1.00, excellent) with 95 % confidence interval (CI) and the Bland–Altman analysis with limits of inter-reader agreement (mean difference ± 1.96 × standard deviation (SD) (18,19) . P values less than 0.05 were considered to represent statistical significance. All statistical analyses were performed using the SPSS software package (SPSS, Chicago, IL).

Results

Seventy-three patients (55 men, 18 women; age 63±9,8 years, ranged between 33 and 82, scanned between January 2014 and November 2016) with pathologically proven primary adenocarcinoma (n = 30) and squamous cell carcinoma (SCC) (n = 43) of the lung were included in this study. There were 6 patients with multiple lung lesions. Only the largest lung lesion was evaluated on MR images. Pathological specimens were obtained through transthoracic or transbronchial biopsy in 48 subjects and 25 patients underwent surgery. In average, MRI was performed in 4.8 days (range 0–12 days) following PET/CT.

As displayed in the scatter plots, significant inverse correlations were found between ADCmin and SUVmax, and ADCmean and SUVmean (Fig. 1A–B).

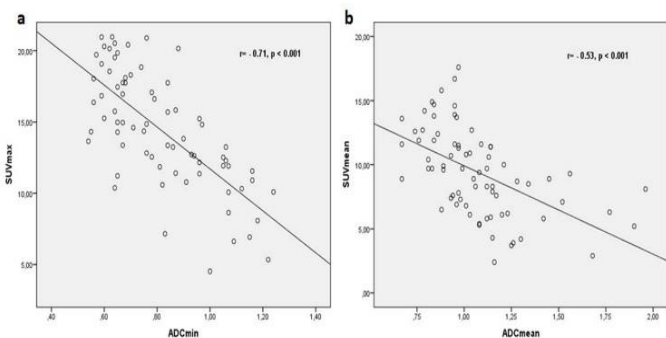


FIGURE 1: A: Scatter plots show a significant inverse correlation between the ADCmin and the SUVmax (r=-0.71; p<0.001) and B: the ADCmean and the SUVmean (r=-0.53; p<0.001).

mean and range of ADC values and SUVs of tumor subtypes are shown in Table 2.

Table 2 . Imaging parameters and tumor subtypes

	Adenocarcinoma	Squamos cell carcinoma	p value
	n= 30	n= 43	
SUV _{max}	13.47±0.67 (12.09-14.85:95% CI)	15.11±0.67 (12.09-14.85: 95% CI)	0.09
SUV _{mean}	8.93±0.59 (7.70-10.15: 95% CI)	9.76±0.52 (8.69-10.83:95% CI)	0.30
ADC _{min} (×10 ⁻³ mm ² /s)	0.82±0.37 (0.90-0.75:95% CI)	0.80±0.29 (0.86-0.74:95% CI)	0.63
ADC _{mean} (×10 ⁻³ mm ² /s)	1.12±0.05 (1.02-1.23:95% CI)	1.03±0.03 (0.95-1.10:95% CI)	0.12

No statistically significant difference was detected between adenocarcinoma and SCC groups.

Fig. 2A–D shows representative images of CT, PET/CT, MRI and ADC map.

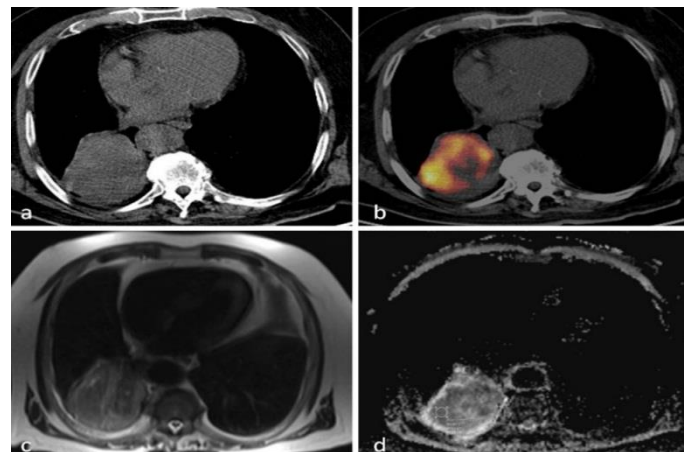


FIGURE 2: A: Axial CT image reveals right lower lobe mass. B: Corresponding PET/CT image at the same image position revealing a maximum SUV of 10.2. C: T2-weighted HASTE MR image revealing a homogenous tumor signal. D: Corresponding ADC map shows low signal intensity at the periphery of the tumor (ADCmin= 0.75 × 10⁻³mm²/s).

The total ICC of 0.747 (95% CI 0.625 to 0.833) and also Blant Altman analysis indicated a good agreement between the two observers for the ADC measurements (Fig. 3).

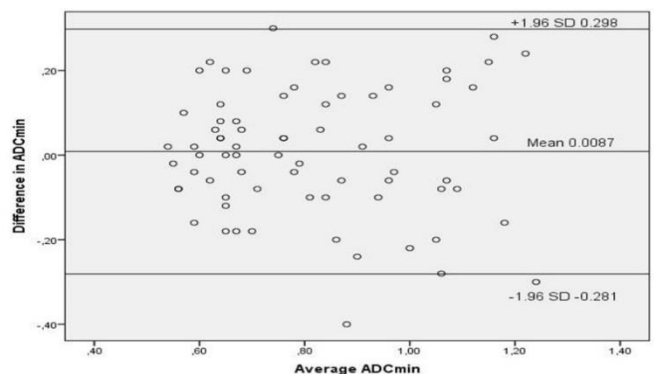


FIGURE 3: Bland-Altman analysis of the difference between ADC_{min} measured by the two observers compared to the average ADC_{min} measured by observer 1.

Discussion

In this study, we found that a significant inverse correlation between SUV and ADC values and a good agreement between observers for ADC measurements in patients with NSCLC. Our results suggest that ADC may be a complementary tool to PET/CT as a functional imaging biomarker for NSCLC patients. Supporting our findings, Ohno et al. (19) reported that ADC and 18F-FDG uptake of the tumor measured before chemoradiotherapy can be used as biomarkers in patients with NSCLC. They even suggested that DWI may be a better modality than PET/CT for prediction of tumor treatment response.

Regier et al. (15) described the inverse correlation of SUV from PET/CT and ADC from DWI in lung cancer for the first time in a study with 41 patients. They found a significant negative correlation between SUV_{max} and ADC_{min} as in our results but SUV_{mean} and ADC_{mean} were not found to be correlated in their study. In a study of NSCLC patients with hybrid 18F-FDG PET/MR, Heusch et al. (16) found significant inverse correlation between ADC_{mean} and SUV_{mean} consistent with our study.

In another PET/MR study of lung lesions, ADC_{min} and SUV_{max} as measures of the cell density and glucose metabolism showed a significant reverse correlation. No significant correlation was found between ADC_{mean} and SUV_{mean} (20). In another study by Mori et al. (21) with 104 patients with pulmonary masses, the ADC_{min} and SUV contrast ratio values had a significant negative correlation. Studies investigating the relationship between ADC value and SUV of non-pulmonary lesions also have varying results. Although there are studies reporting significant negative correlation between ADC value and SUV in brain tumors, rectal cancer, gastrointestinal stromal tumor, pancreatic adenocarcinoma, and head and neck carcinoma (22-26), no such a correlation was shown in B-cell lymphomas, primary cervical cancer, and breast cancer (27-30). We believe that these inconsistent results are due to tumor heterogeneity and different ROI drawing methods for ADC measurements. Drawing ROI on more than one slice, expanding the ROI to encompass the entire tumor and measuring the volumetric ADC value of the tumor cause significantly different results particularly in heterogeneous masses. OSR method was found to be the fastest and easiest method with the excellent inter-observer agreement in a study comparing five different methods of region-of-interest positioning (17). Thus, we measured both ADC value and SUV on the same slice on which the longest diameter of the tumor is seen and an OSR ROI was placed on the area on the ADC map corresponding to the area with the highest SUV on visual evaluation of the PET/CT images. We paid special attention to confine the ROI on the area with the most apparent diffusion restriction. We believe that the fact that we have found a significant correlation between ADC_{mean} and SUV_{mean} unlike in other

studies is related to our measurement method.

PET/CT has become the modality of choice in the diagnosis, staging and follow up of NSCLC due to the information it provides about the morphologic and metabolic features of the tumor tissue (31). The majority of lung cancers have high glucose affinity as other malignant tumors. SUV is a significant semi-quantitative biomarker which reflects glucose metabolism and indirectly tumor cellularity (32). In previous studies, 18F-FDG uptake of the tumor and prognosis were found to be strongly associated (33). In a multivariate analysis of 155 patients with NSCLC, Ahuja et al. (34) found that an SUV level greater than 10 provides most valuable prognostic information independent of clinical stage and lesion size. Thus, it has been reported that standard 18F-FDG uptake is an important prognostic factor in NSCLC (35).

On the other hand, DWI is an MRI technique that can measure the diffusion of water molecules in biological tissues quantitatively and noninvasively and it is being used more extensively in oncologic imaging. The movement of water molecules outside the body is not restricted and called as 'free diffusion'. However, their *in vivo* movements are hindered due to macromolecules and cell membranes. Diffusion restriction is more prominent in hypercellular tissues. On the contrary, diffusion restriction is less apparent in hypocellular tissues, tissues with large extracellular space, and when cell membrane integrity is compromised. The quantitative assessment of diffusion is made on ADC maps which show the amount of diffusion of water molecules (36). High ADC values indicate normal or increased diffusion and are seen in healthy tissues or benign pathologies with large extracellular space and low cellular density. Low ADC values indicate diffusion restriction and are associated with hypercellularity, cytotoxic edema or dense contents (hemorrhage, protein). Increased cell number and nucleus/cytoplasm ratio, accumulation of macromolecules, and shrinkage of the extracellular space impede movements of the water molecules and cause diffusion restriction in malignant masses. Previous studies have shown that highly cellular tumors are associated with more apparent diffusion restriction and lower ADC values (37,38).

The theory that there may be a correlation between SUV_{max} which reflects the metabolic activity and cell proliferation of the tumor and ADC value which is a measurement of the diffusion restriction of water molecules in the tumor tissue caused by the increase in number and size of the tumor cells is yet to be proven.

DWI has some significant advantages over other diagnostic methods such as CT, PET, or biopsy. No ionizing radiation exposure and no contrast material requirement, non-invasiveness, shorter acquisition time, and repeatability are among these advantages.

This study has some limitations. First, the patient population was relatively small and only two lung cancer subgroups were evaluated. However, we found some significant correlations

between ADC and SUV parameters. Second, we didn't perform survival analysis to assess predictive capabilities of DWI and PET/CT. Third, the correlation between pathological grade of the tumor which is an important prognostic factor and SUV or ADC was not evaluated. Future studies investigating this correlation may show the relationship between tumor cellularity and SUV or ADC more clearly. Fourth, we didn't use relative ADC values which are calculated by the formula $ADC_{lesion}/ADC_{reference}$ site (28), instead, we used simple ADC values which can be obtained easily in routine clinical practice (17).

Conclusion

Our results show that there is a significant inverse correlation between ADC values obtained from DWI and SUVs from PET/CT. The presence of a correlation between tumor glucose metabolism and tumor cellularity might improve the characterization and the perception of biological properties of NSCLC. Thus, ADC value might prove to serve as a biomarker similar to SUV in functional imaging of lung cancer. However, further large prospective comparative studies investigating the prognostic significance and predictive ability of DWI in treatment response are needed to integrate DWI into the daily clinical management of NSCLC patients.

References

- [1] Torre LA, Bray F, Siegel RL, Ferlay J, Lortet-tieulent J, Jemal A. Global Cancer Statistics, 2012. CA: a cancer J Clin. 2015;65:87-108.
- [2] McMahon PM, Kong CY, Johnson BE, Weinstein MC, Weeks JC, Kuntz KM, et al. Estimating Long-term Effectiveness of Lung Cancer Screening in the Mayo CT Screening Study. Radiology. 2008;248(1):278-87.
- [3] Volm M, Koomägi R. Relevance of proliferative and pro-apoptotic factors in non-small-cell lung cancer for patient survival. Br J Cancer. Nature Publishing Group; 2000 May;82(10):1747-54.
- [4] Wigren T. Confirmation of a prognostic index for patients with inoperable non-small cell lung cancer. Radiother Oncol. 1997;44(1):9-15.
- [5] Hellwig D, Groschel A, Graeter TP, Hellwig AP, Nestle U, Schafers H-J, et al. Diagnostic performance and prognostic impact of FDG-PET in suspected recurrence of surgically treated non-small cell lung cancer. Eur J Nucl Med Mol Imaging. Germany; 2006;33:13-21.
- [6] Patz EF, Connolly J, Herndon J. Prognostic value of thoracic FDG PET imaging after treatment for non-small cell lung cancer. AJR Am J Roentgenol. 2000;174:769-74.
- [7] Cerfolio RJ, Bryant AS, Ohja B, Bartolucci AA. The maximum standardized uptake values on positron emission tomography of a non-small cell lung cancer predict stage, recurrence, and survival. J Thorac Cardiovasc Surg. United States; 2005;130:151-9.
- [8] Chung HW, Lee KY, Kim HJ, Kim WS, So Y. FDG PET/CT metabolic tumor volume and total lesion glycolysis predict prognosis in patients with advanced lung adenocarcinoma. J Cancer Res Clin Oncol. 2014;140:89-98.
- [9] Vesselle H, Freeman JD, Wiens L, Stern J, Nguyen HQ, Hawes SE, et al. Fluorodeoxyglucose Uptake of Primary Non-Small Cell Lung Cancer at Positron Emission Tomography: New Contrary Data on Prognostic Role. Clin Cancer Res. 2007;13:3255-63.
- [10] Chang SC, Lai PH, Chen WL, Weng HH, Ho JT, Wang JS, et al. Diffusion-weighted MRI features of brain abscess and cystic or necrotic brain tumors: comparison with conventional MRI. Clin Imaging. 2002;26:227-36.
- [11] McVeigh PZ, Syed AM, Milosevic M, Fyles A, Haider MA. Diffusion-weighted MRI in cervical cancer. Eur Radiol. 2008;18:1058-64.
- [12] Dorenbeck U, Butz B, Schlaier J, Bretschneider T, Schuierer G, Feuerbach S. Diffusion-weighted echo-planar MRI of the brain with calculated ADCs: a useful tool in the differential diagnosis of tumor necrosis from abscess? J Neuroimaging. 2003;13:330-8.
- [13] Matoba M, Tonami H, Kondou T, Yokota H, Higashi K, Toga H, et al. Lung carcinoma : Diffusion-weighted MR Imaging — preliminary evaluation with apparent diffusion coefficient. Radiology. 2007;243:570-7.
- [14] Coolen J, Vansteenkiste J, De Keyzer F, Decaluwé H, De Wever W, Deroose C, et al. Characterisation of solitary pulmonary lesions combining visual perfusion and quantitative diffusion MR imaging. Eur Radiol. 2014;24:531-41.
- [15] Regier M, Derlin T, Schwarz D, Laqmani A, Henes FO, Groth M, et al. Diffusion weighted MRI and 18F-FDG PET/CT in non-small cell lung cancer (NSCLC): does the apparent diffusion coefficient (ADC) correlate with tracer uptake (SUV)? Eur J Radiol. Ireland; 2012;81:2913-8.
- [16] Heusch P, Buchbender C, Kohler J, Nensa F, Beiderwellen K, Kuhl H, et al. Correlation of the apparent diffusion coefficient (ADC) with the standardized uptake value (SUV) in hybrid 18F-FDG PET/MRI in non-small cell lung cancer (NSCLC) lesions: initial results. Rofo. Germany; 2013;185:1056-62.
- [17] Priola AM, Priola SM, Parlatano D, Gned D, Giraudo MT, Giardino R, et al. Apparent diffusion coefficient measurements in diffusion-weighted magnetic resonance imaging of the anterior mediastinum: inter-observer reproducibility of five different methods of region-of-interest positioning. Eur Radiol. European Radiology; 2016;1-9.
- [18] Bland JM, Altman DG. Statistical Methods for Assessing Agreement Between Two Methods of Clinical Measurement. Lancet. 1986;327:307-10.
- [19] Ohno Y, Koyama H, Yoshikawa T, Matsumoto K,

Aoyama N, Onishi Y, et al. Diffusion-weighted MRI versus 18F-FDG PET/CT: performance as predictors of tumor treatment response and patient survival in patients with non-small cell lung cancer receiving chemoradiotherapy. *AJR Am J Roentgenol.* United States; 2012;198(1):75–82.

[20] Schmidt H, Brendle C, Schraml C, Martirosian P, Bezrukov I, Hetzel J, et al. Correlation of simultaneously acquired diffusion-weighted imaging and 2-deoxy-[18F] fluoro-2-D-glucose positron emission tomography of pulmonary lesions in a dedicated whole-body magnetic resonance/positron emission tomography system. *Invest Radiol.* United States; 2013 May;48(5):247–55.

[21] Mori T, Nomori H, Ikeda K, Kawanaka K, Shiraishi S, Katahira K, et al. Diffusion-weighted magnetic resonance imaging for diagnosing malignant pulmonary nodules/masses: comparison with positron emission tomography. *J Thorac Oncol.* 2008;3(4):358–64.

[22] Palumbo B, Angotti F, Marano GD. Relationship between PET-FDG and MRI apparent diffusion coefficients in brain tumors. *Q J Nucl Med Mol Imaging.* 2009;53:17-22.

[23] Gu J, Khong P-L, Wang S, Chan Q, Law W, Zhang J. Quantitative Assessment of Diffusion-Weighted MR Imaging in Patients with Primary Rectal Cancer: Correlation with FDG-PET/CT. *Mol Imaging Biol.* 2011;13:1020-28.

[24] Wong CS, Gong N, Chu YC, Anthony MP, Chan Q, Lee HF, et al. Correlation of measurements from diffusion weighted MR imaging and FDG PET/CT in GIST patients: ADC versus SUV. *Eur J Radiol.* 2012;8:2122-6.

[25] Sakane M, Tatsumi M, Kim T, Hori M, Onishi H, Nakamoto A, et al. Correlation between apparent diffusion coefficients on diffusion-weighted MRI and standardized uptake value on FDG-PET/CT in pancreatic adenocarcinoma. *Acta Radiol.* 2015;56:1034-41.

[26] Nakajo M, Nakajo M, Kajiya Y, Tani A, Kamiyama T, Yonekura R, et al. FDG PET/CT and diffusion-weighted imaging of head and neck squamous cell carcinoma: comparison of prognostic significance between primary tumor standardized uptake value and apparent diffusion coefficient. *Clin Nucl Med.* 2012;37:475-80.

[27] de Jong A, Kwee TC, de Klerk JM, Adam J a, de Keizer B, Fijnheer R, et al. Relationship between pretreatment {FDG-PET} and diffusion-weighted {MRI} biomarkers in diffuse large B-cell lymphoma. *Am J Nucl Med Mol Imaging.* 2014;4:231-8.

[28] Wu X, Korkola P, Pertovaara H, Eskola H, Järvenpää R, Kellokumpu-Lehtinen PL. No correlation between glucose metabolism and apparent diffusion coefficient in diffuse large B-cell lymphoma: A PET/CT and DW-MRI study. *Eur J Radiol.* 2011;79:e117-e121.

[29] Ho KC, Lin G, Wang JJ, Lai CH, Chang CJ, Yen TC. Correlation of apparent diffusion coefficients measured by 3T diffusion-weighted MRI and SUV from FDG PET/CT in

primary cervical cancer. *Eur J Nucl Med Mol Imaging.* 2009;36:200-8.

[30] Nakajo M, Kajiya Y, Kaneko T, Kaneko Y, Takasaki T, Tani A, et al. FDG PET/CT and diffusion-weighted imaging for breast cancer: prognostic value of maximum standardized uptake values and apparent diffusion coefficient values of the primary lesion. *Eur J Nucl Med Mol Imaging.* 2010;37:2011-20.

[31] Fischer B, Lassen U, Mortensen J, Larsen S, Loft A, Bertelsen A, et al. Preoperative staging of lung cancer with combined PET-CT. *N Engl J Med.* 2009;361:32-39.

[32] Rakheja R, Chandarana H, DeMello L, Jackson K, Geppert C, Faul D, et al. Correlation between standardized uptake value and apparent diffusion coefficient of neoplastic lesions evaluated with whole-body simultaneous hybrid PET/MRI. *Am J Roentgenol.* 2013;201:1115-9.

[33] Detterbeck FC, Vansteenkiste JF, Morris DE, Doooms CA, Khandani AH, Socinski MA. Seeking a home for a PET, part 3: Emerging applications of positron emission tomography imaging in the management of patients with lung cancer. *Chest.* 2004;126:1656-66.

[34] Ahuja V, Coleman RE, Herndon J, Patz EFJ. The prognostic significance of fluorodeoxyglucose positron emission tomography imaging for patients with nonsmall cell lung carcinoma. *Cancer.* United States; 1998;83:918–24.

[35] Borst GR, Belderbos JSA, Boellaard R, Comans EFI, De Jaeger K, Lammertsma AA, et al. Standardised FDG uptake: a prognostic factor for inoperable non-small cell lung cancer. *Eur J Cancer.* 2005;4:1533-41.

[36] Bammer R. Basic principles of diffusion-weighted imaging. *Eur J Radiol.* 2003;45:169-84.

[37] Herneth AM, Guccione S, Bednarski M. Apparent diffusion coefficient: a quantitative parameter for in vivo tumor characterization. *Eur J Radiol.* 2003;4:208-13.

[38] Hayashida Y, Hirai T, Morishita S, Kitajima M, Murakami R, Korogi Y, et al. Diffusion-weighted imaging of metastatic brain tumors: comparison with histologic type and tumor cellularity. *Am J Neuroradiol.* 2006;27:1419-25.